Available online at www.sciencedirect.com

SCIENCE DIRECT®

Journal of Photochemistry and Photobiology A: Chemistry 175 (2005) 39–44

Journal of Photochemistry and Photobiology A:Chemistry

www.elsevier.com/locate/jphotochem

New branched hydrazones as hole transporting materials

V. Getautis [a,*], M. Daskeviciene [a], V. Gaidelis [b], V. Jankauskas [b]

[a] *Department of Organic Chemistry, Kaunas University of Technology, Radvilenu pl. 19, LT-50270 Kaunas, Lithuania*
[b] *Department of Solid State Electronics, Vilnius University, Saulėtekio 9, LT-10222 Vilnius, Lithuania*

Received 7 January 2005; accepted 12 April 2005

Abstract

The new hole transporting materials with molecules consisting of two hydrazone branches linked with flexible benzene ring and two hydroxyl groups containing central bridge were synthesized and investigated. These transporting materials are low molecular glasses and allow preparing stable to crystallization layers. Ionisation potential of the materials is in the range 5.04–5.43 eV. The highest hole mobility, reaching 10^{-4} cm^2/V s at 6×10^5 V/cm electric field, was observed in the transporting material with triphenylamine moiety. These transporting materials can be used with or, in the case of a solid substrate, without binder polymer.

Keywords: Conducting materials; Hole drift mobility; Hydrazones; Molecular glasses

---

1. Introduction

Aromatic hydrazone molecules dispersed in a binder polymer (BM) are used as the main constituent of electrophotographic devices due to their excellent hole-transporting properties and relatively simple synthesis [1–4]. The presence of large proportion of BM in the electrophotographic layers (EPL), usually 50% of the total composition mass leads to considerable decrease of carrier mobility. Even in such compositions, possibility of the transporting material (TM) crystallization remains and causes problems during EPL preparation and long application, because low-molecular-weight hydrazones generally tend to form crystals. It is of interest and significance to develop photo- and electroactive low-molecular-weight amorphous materials that form stable amorphous glasses having glass-transition temperatures above room temperature. These molecular glasses will form stable films without BM, and are expected to manifest properties and functions more effectively relative to molecularly doped polymer compositions. Among the great number of studies devoted to low-molar-mass aromatic hydrazones only few glass-forming compounds with hydrazone moiety are reported [5–8]. Another problem, which arises with preparation of the belt format EPL on flexible supports, is bending and stretching stability of the layers. This problem is especially acute in the machines with liquid development, because liquid developer promotes crack formation. Solving these problems requires new TM with special molecule design and improved properties.

We have reported on novel class of well-defined molecular glasses, obtained in the reactions of oxiranes containing photoconductive groups with different bifunctional nucleophylic compounds, such as aromatic diols, dimercapto compounds, derivatives of aniline [9–12]. The existence of several diastereoisomers, the possibility of intermolecular hydrogen bonding and flexibility of aliphatic linking chains ensure high morphological stability of these glasses. In the present article we report on new, branched hydrazone derivatives as hole transporting materials. The molecules of these TM consist of two hydrazone branches linked by the central flexible benzene ring containing bridge. The molecular structure of these TM makes crystallisation in solid state difficult, so these materials are low molecular glasses. Another peculiarity of these TM is presence of two hydroxyl groups in molecule. This improves adhesion and compatibility with various BM,

---

[*] Corresponding author. Tel.: +370 37 300196; fax: +370 37 300152.
E-mail address: vgetaut@ktu.lt (V. Getautis).

1010-6030/$ – see front matter © 2005 Elsevier B.V. All rights reserved.
doi:10.1016/j.jphotochem.2005.04.032

including polycarbonate (PC) and polyvinylbutyral (PVB). These TM can be used with binder, without binder in the case of solid substrate, or with low binder concentrations. They can be chemically cross-linked in the layer by reaction of the hydroxyl groups with polyisocyanates [14].

2. Experimental details

2.1. Preparation of the branched hydrazones (Scheme 1)

2,3-Epoxypropyl derivatives of phenylhydrazones were prepared according to our earlier procedure [13]. The synthesis of the branched hydrazones **H1**–**H7** was carried out to the following procedure [11].

The corresponding 2,3-epoxypropyl derivative of phenylhydrazone (27.1 mmol) and corresponding benzenediol (12.3 mmol) were dissolved in 15 ml of butanone, and 2 ml of a catalyst triethylamine (TEA) were added. The obtained mixture was refluxed until the benzenediol and its monosubstituted derivative disappeared (10–14 h). At the end of the reaction (TCL control, ether–hexane, 3:1) butanone and TEA were distilled off and the residue was dissolved in toluene. The separated crystalline products **H5**–**H7** were filtered off. Compounds **H1**–**H4** were purified by column chromatography using propanone–hexane (1:4) as the eluent.

The details of synthesis and spectral data of **H1**–**H6** are reported in Ref. [11]. The yield of **H7** was 8.9 g (76%), m.p. 109–110.5 °C (toluene). ^{1}H NMR spectrum ($CDCl_3$): 7.63 (2H, s, CH=N); 7.50–7.0 (37H, m, Ar); 6.96 (2H, t, $J = 7.3$ Hz, 4-H Ph); 6.55 (2H, d, $J = 7.9$ Hz, 4-H, 6-H of m-Ph); 6.51 (1H, s, 2-H of m-Ph); 4.40 (2H, p, $J = 5.5$ Hz, CH); 4.18 (2H, dd, part of the ABX system, H_A of NCH_2, $J_{AB} = 14.7$ Hz, $J_{AX}=6.1$ Hz); 4.04 (6H, m, H_B of NCH_2, CH_2O); 2.86 ppm (2H, d, $J = 5.5$ Hz, OH). Found, %: C 78.46; H 5.95; N 8.85. $C_{62}H_{56}N_6O_4$. Calculated, %: C 78.26; H 5.89; N 8.99.

2.2. Measurement

The ^{1}H NMR spectrum was taken on a Mercury-VX (400 MHz) spectrometer with TMS as the internal standard. The UV spectra were recorded on a Spectronic Genesys 8 spectrometer in acetonitrile. 10^{-4} M solution of investigated TM and micro cell with an internal width of 1 mm was used. The phase transitions of **H1**–**H7** were investigated by the differential scanning calorimetry (DSC) method on Perkin Elmer DSC-7 apparatus. Samples of 3–12 mg as obtained from synthesis were heated in aluminium pans at a scan rate 10 K/min under a nitrogen flow. During the first heating the melting points were measured. After melting, the samples were cooled with the same rate. The resulting glasses were heated again under the same conditions to measure the glass transitions.

Table 1
Composition and parameters of the branched hydrazones **H1**–**H7**

TM	Substituted benzene	*R*	T_m (°C)	T_g (°C)	I_P (eV)
H1	1,2-	**a**	–	46	5.04
H2	1,3-	**a**	60	51	5.11
H3	1,4-	**a**	67	58	5.11
H4	1,2-	**b**	–	78	
H5	1,3-	**b**	145	80	5.35
H6	1,4-	**b**	214	89	
H7	1,3-	**c**	89; 106	82	5.43

The samples for mobility measurements were prepared with most of the TM listed in Table 1, with the exception of **H6**, which was nearly insoluble. The branched hydrazones are able to form stable layers without binder, so samples for mobility measurements were prepared from neat TM and from 1:1 mass proportion compositions of TM with various binders. PVB1 from Aldrich PVB 41,843-9 with average $M_W = 70{,}000–100{,}000$ and 18–20 wt.% of hydroxyl groups; and PC-Z from Mitsubishi Gas Chemical Co. polycarbonate Iupilon Z-200 were used as BM. The samples for mobility measurements were prepared by coating TM solutions or solutions of the TM compositions with binder in THF on polyester film with conductive Al layer. The layer thickness was in the range 5–10 μm.

The hole drift mobility was measured by xerographic time of flight technique (XTOF) [15–17]. Positive corona charging created electric field inside the TM layer. Charge carriers were generated at the layer surface by illumination with pulses of nitrogen laser (pulse duration was 2 ns, wavelength 337 nm). The layer surface potential decrease as a result of pulse illumination was up to 1–5% of initial potential before illumination. The capacitance probe that was connected to the wide frequency band electrometer measured the speed of the surface potential decrease dU/dt. The transit time t_t was determined by the kink on the curve of the dU/dt transient in linear scale. The drift mobility was calculated by the formula $\mu = d^2/U_0 t_t$, where d is the layer thickness and U_0 is the surface potential at the moment of illumination.The ionisation potential I_p was measured by the electron photoemission in air method, similar to the used in [18] and described in [19].

3. Results and discussion

The general route to the branched hydrazone derivatives including diethylaniline (**H1**–**H3**), ethylcarbazole (**H4**–**H6**), triphenylamine (**H7**) moieties is shown in Scheme 1. These compounds were prepared by the reaction of various benzenediols with 2 equivalents of corresponding aryl- or hetero-aryl aldehyde phenylhydrazone *N*-2,3-epoxypropyl derivative in the presence of catalyst TEA. The synthesized branched hydrazones consisting of two hydrazone branches linked with flexible benzene ring and two hydroxyl groups containing central bridge are low molecular glasses and have been found to exhibit glass-transition phenomena usually associated with polymers. In contrast to amorphous polymers the branched

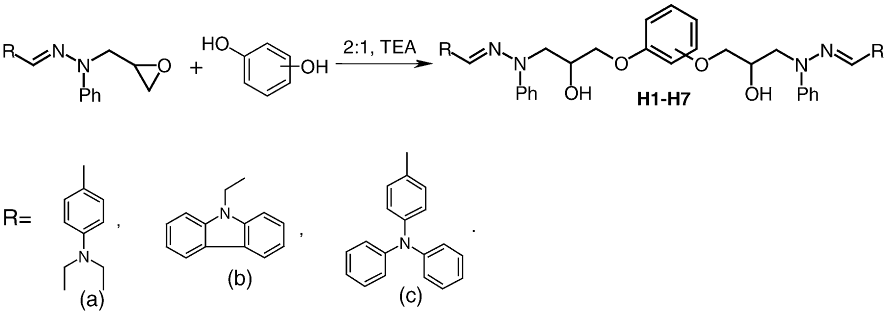

Scheme 1. Synthesis route of the branched hydrazones **H1**–**H7**.

hydrazones are pure materials with well-defined molecular structures and definite molecular weights without any distribution. They were identified by IR, UV, NMR spectroscopy and elemental analysis.

Formation of the glassy state of **H1**–**H7** was confirmed by DSC analysis. The melting points (T_m) and glass transition temperatures (T_g) of synthesized TM are presented in Table 1. These investigations revealed that some of the branched hydrazones could exist both in crystalline and amorphous state while others were found only in amorphous phase in our experiments. The DSC curve for **H6** at first heating reveals a number of polymorphous changes before melting at 214 °C (Fig. 1). No crystallization takes place during cooling or second heating, only glass transition at 89 °C is revealed in the second heating. This means that the material remains in glassy state after melting and subsequent cooling. This is common feature for all the branched hydrazones investigated here. The glassy state of these materials is quite stable; no signs of crystallization were detected in the glassy layers during over year storage at ambient conditions. Glass transition occurs at 78 °C but no melting is seen for **H4** (Fig. 2), this means that the original state of the sample was amorphous.

The comparison of the DSC analysis results for the **H4**–**H6** reveals a significant role of the substitution of benzene at the central connecting group. In the case of *para* substitution in **H6**, the melting point is over 200 °C and the material is polymorphic. The melting enthalpy is high, the material is practically insoluble in common organic solvents, except highly polar solvents such as dimethyl formamide. On the other hand **H4** with *ortho* substituted benzene ring was found only in amorphous state and its glass transition point is lower than that of **H6**. These facts indicate significance of the molecule symmetry.

The structure of the charge transporting chromophores also has significant influence on melting, glass transition points and solubility of the synthesized TM. As seen from Table 1, these temperatures are lower for the TM with chromophores **a** as compared with others. TM with triphenylamine chromophore (**c**) has two melting points. This means that there are different crystalline forms of this TM and transitions of one into another take place during first heating. The branched hydrazone **H3** comprising diethylaniline chromophore is soluble in common organic solvents while **H6** was nearly insoluble.

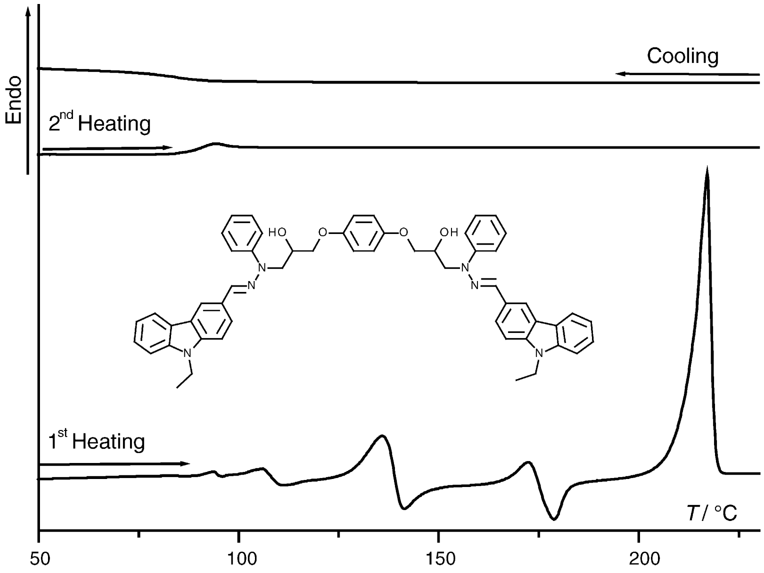

Fig. 1. DSC curves of **H6** (heating and cooling rate 10 K/min).

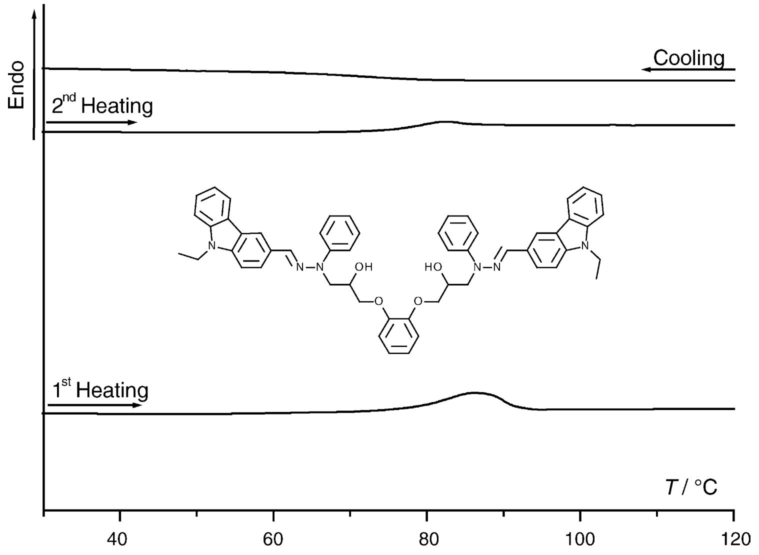

Fig. 2. DSC curves of **H4** (heating and cooling rate 10 K/min).

Since π-electrons are very important for the charge transporting process in TM structures, their state was explored from the light absorption spectra. The largest shift of absorption to longer wavelengths due to conjugated π-electrons for branched hydrazones with triphenylamine moiety **H7** was observed in UV spectra (Fig. 3). On the other hand, diethylaniline containing hydrazones (**H1**–**H3**) exhibit batochromic shift as compared with ethylcarbazole (**H5**) chromophores containing branched hydrazone. In addition, the influence of the central linking fragment on the electron energy of charge transporting molecule is weak in comparison with that of chromophores (comparison **H1**, **H2** and **H3**).

The photoemission in air spectra for some of the branched hydrazones are shown on Fig. 4, ionization potential values are presented in Table 1. There is little ionization potential (I_p) difference depending on the central connecting group, the charge transporting groups are determining its value. The lowest I_p values, about 5.1 eV, were observed in the TM with chromophore with diethylaniline group (**a**). Replacement of this group by ethylcarbazole (**b**) or triphenylamine (**c**) group leads to increase of I_p by more than 0.25 eV.

XTOF measurements revealed that small charge transport transients are Gaussian with well-defined transit time on linear plots in all the cases investigated both for the samples of pure TM or compositions of them with various BM. This is illustrated on Fig. 5.

Examples of mobility field dependencies are given in Figs. 6 and 7. In all the cases investigated, the mobility μ is approximated by the formula

$$\mu = \mu_0 \exp(\alpha\sqrt{E}) \qquad (1)$$

where μ_0 is the zero field mobility, α is Pool–Frenkel parameter, and E is electric field strength. The mobility defining parameters μ_0 and α values as well as the mobility value at the 6.4×10^5 V/cm field strength are given in Table 2.

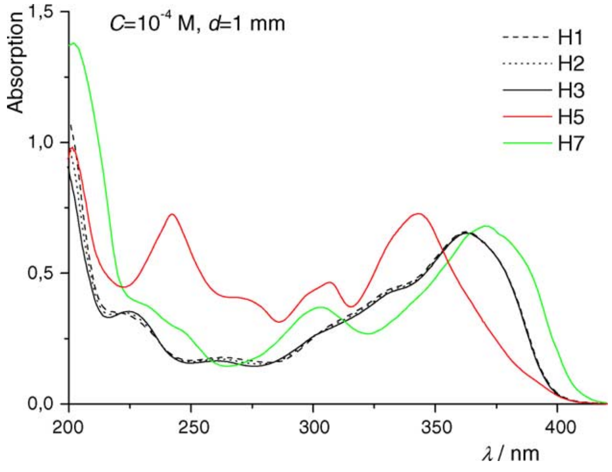

Fig. 3. Light absorption spectra of the branched hydrazones **H1**–**H3**, **H5**, **H7** in acetonitrile.

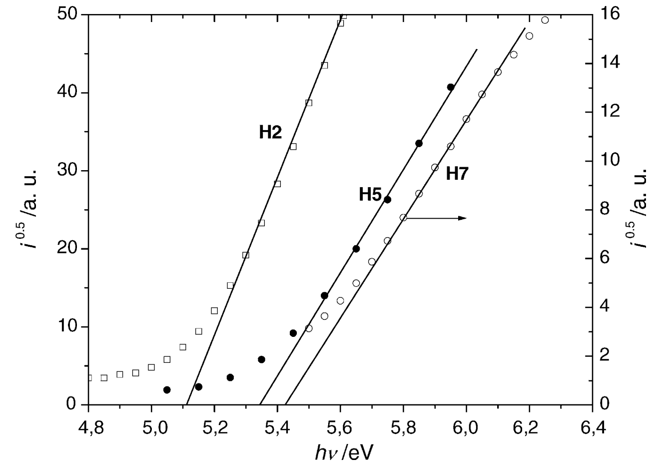

Fig. 4. Photoelectron emission in air spectra of the **H2**, **H5**, **H7**.

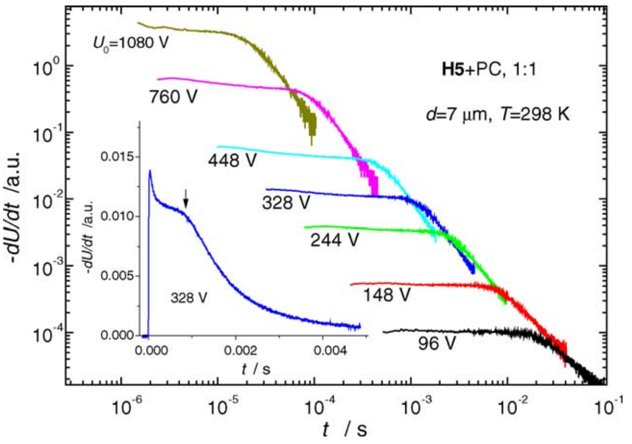

Fig. 5. XTOF transients for **H5** 1:1 composition with PC. Insert shows a typical transient curve in linear plot.

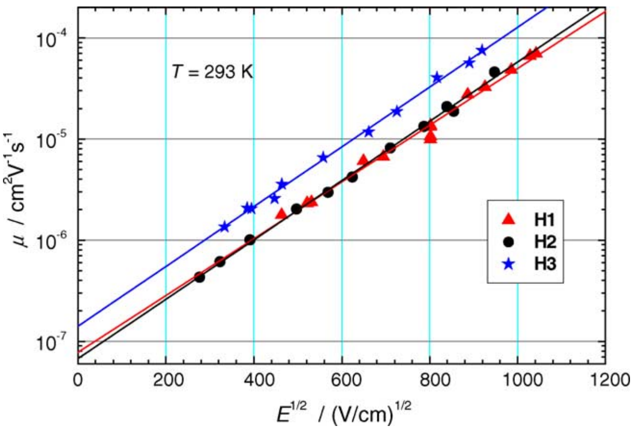

Fig. 6. Mobility field dependencies for pure **H1**–**H3**.

Table 2
Mobility data

Layer composition	μ_0 (cm^2/V s)	μ (cm^2/V s)	α (cm/V)$^{0.5}$
H1	8.0×10^{-8}	1.4×10^{-5}	0.0065
H2	7.0×10^{-8}	1.5×10^{-5}	0.0068
H3	1.3×10^{-7}	3.3×10^{-5}	0.0068
H5	1.5×10^{-7}	2.0×10^{-5}	0.0061
H5 + PC, 1:1	5.3×10^{-8}	3.5×10^{-6}	0.0053
H5 + PVB, 1:1	6.0×10^{-9}	7.5×10^{-7}	0.0061
H7	2.4×10^{-6}	1.3×10^{-4}	0.0050

As seen from the results presented the mobility value is influenced by the charge transporting chromophore nature. The highest mobility values are with chromophores based on triphenylamine (**H7**). This is natural because conjugated π-electron systems are largest in this chromophore. The lowest mobility was found in the case of the branched hydrazones with diethylaniline groups. However, there is a small difference of mobility at strong electric fields between the branched hydrazones containing diethylaniline and carbazole chromophores. The central linking fragment also conditions hole mobility; however, this influence is much weaker in comparison with that of chromophores. It is seen from comparison of mobility points for hydrazones linked by 1,2-, 1,3- and 1,4-benzenediols in Fig. 6, that values are highest for the most symmetrical compound **H3** as compared to **H1** and **H2**. This can be explained assuming that molecular symmetry causes the decrease of the charge carrier trapping centres concentration.

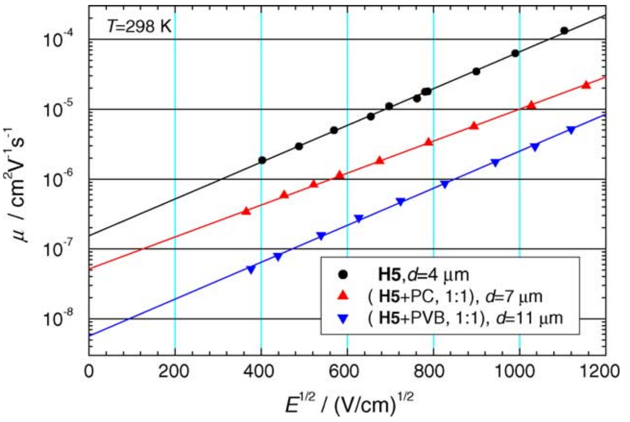

Fig. 7. Mobility field dependencies for pure **H5** and its 1:1 compositions with various BM.

Mobility in the compositions of TM with BM is considerably lower as compared with neat TM. The difference makes up to two orders of magnitude. The highest mobility among the **H5** compositions, as one can see from Fig. 7 and Table 2, is in the case of polycarbonate BM. Mobility in this case is by one order of magnitude higher than in compositions with PVB. The hydroxyl groups present in PVB, probably, cause this. However, special properties of PVB due to presence of hydroxyl groups, such as good adhesion, stability to bending and stretching and effects of liquid developer may outweigh loss of mobility.

References

[1] N. Mori, U.S. Patent No. 5,567,557 (1996).
[2] N. Tatsya, U. Minoru, Japan Patent No. 8,101,524 (1996).
[3] Y. Suzuki, U.S. Patent No. 5,665,500 (1997).
[4] N. Jubran, Z. Tokarski, T.P. Smith, U.S. Patent No. 6,340,548 (2002).
[5] K.J. Jiang, Y.L. Sun, K.F. Shao, L.M. Yang, Chem. Lett. 33 (2004) 50–51.
[6] H. Nam, D.H. Kang, J.K. Kim, S.Y. Park, Chem. Lett. 11 (2000) 1298–1299.
[7] P.M. Borsenberger, Adv. Mater. Opt. Electr. 1 (1992) 73–80.
[8] K. Nishimura, H. Inada, T. Kobata, Y. Matsui, Y. Shirota, Mol. Cryst. Liq. Cryst. 217 (1992) 235–242.
[9] S. Kutkevicius, A. Stanisauskaite, V. Getautis, A. Railaite, J. Prakt. Chem. 337 (1995) 315–318.
[10] M. Daskeviciene, V. Gaidelis, V. Getautis, V. Jankauskas, O. Paliulis, J. Sidaravicius, Lithuanian J. Phys. 41 (2001) 521–526.
[11] V. Getautis, M. Daskeviciene, A. Stanisauskaite, O. Paliulis, Chemistry of Heterocyclis Compounds 7 (2002) 884–888.
[12] V. Getautis, O. Paliulis, I. Paulauskaite, V. Gaidelis, V. Jankauskas, J. Sidaravicius, Z. Tokarski, K. Law, N. Jubran, J. Imag. Sci. Technol. 48 (2004) 265–272.
[13] A. Stanisauskaite, V. Getautis, A. Railaite, Chemija 3 (1996) 68–73.

[14] V. Gaidelis, J. Gavutiene, V. Getautis, J.V. Grazulevicius, V. Jankauskas, R. Kavaliunas, R. Lazauskaite, O. Paliulis, M.A. Rossman, D.J. Sidaravicius, T.P. Smith, A. Stanisauskaite, U.S. Patent No. 6,214,503 (2001).

[15] E. Montrimas, V. Gaidelis, A. Pazera, Lithuanian J. Phys. 6 (1966) 569–576.

[16] S.M. Vaezi-Nejad, Int. J. Electron. 62 (1987) 361–384.

[17] Y.C. Archie, C. Chan, Juhasz, Int. J. Electron. 62 (1987) 625–632.

[18] E. Miyamoto, Y. Yamaguchi, M. Yokoyama, Electrophotography 28 (1989) 364–370.

[19] M. Daskeviciene, V. Getautis, J.V. Grazulevicius, A. Stanisauskaite, J. Antulis, V. Gaidelis, V. Jankauskas, J. Sidaravicius, J. Imaging Sci. Technol. 46 (2002) 467–472.